

# A Flow Method for Measuring Transport Properties at Flame Temperatures

GEORGE EMBER, J. R. FERRON, and KURT WOHL

University of Delaware, Newark, Delaware

A dynamic diffusion experiment, in which the spread of a tracer material in a laminar stream is followed by appropriate sampling and analytical means, should be well suited for use at high temperatures. Compared with static methods of the Loschmidt type, which have been used at high temperatures in one investigation (1), the dynamic method permits a wider choice of construction materials and shortens significantly the time period required for an experiment.

The advantages of the dynamic method were pointed out by Walker and Westenberg (2) who used the technique for measurements of binary diffusion coefficients up to 1,150°K. These workers preheated the main gas stream to the temperature of the experiment and then made the stream laminar by passing it through a series of screens. They admitted tracer gas through a capillary tube pointed in the direction of flow, sampled downstream with a similar capillary, and analyzed their samples by thermal conductivity methods.

Two significant modifications of this scheme are made in the work described here. The hot, laminar gas stream is composed of the combustion products from a thin, flat flame which burns at the base of the apparatus. This permits investigations at higher temperatures because materials problems involved in preheating the gas and making the flow laminar are avoided. The present method also uses radioactive tracer techniques for analysis. This makes possible the measurement of self-diffusion coefficients as well as binary diffusion coefficients and permits extensive cross checking of diffusion phenomena in multicomponent gas mixtures.

A brief description of the apparatus, together with self-diffusion data for carbon dioxide at 1,180° to 1,680°K. has been given previously (3). The purpose of this paper is to present a fuller discussion of the construction features of the apparatus and of recent modifications of the apparatus and the method. Self-diffusion and binary diffusion data for the carbon dioxide-methane system at 1

atm. and 297°K. are given. A portion of the results of an investigation of the system carbon dioxide-water at 1 atm. and 975° to 1,616°K. is also included.

## EXPERIMENTAL APPARATUS

The general features and overall dimensions of the main parts of the apparatus are indicated schematically in Figure 1. The four principal parts shown are the flat-flame burner, the measuring section, the probe-inlet section, and the cooling and gas-discharge section. Auxiliary equipment, not indicated in Figure 1, includes metering devices for fuel, oxidant, diluent gas, and tracer gas; gas-sampling pump and radioactivity detection system; temperature-measuring equipment; and electrical supply systems for the heating coils in the measuring section.

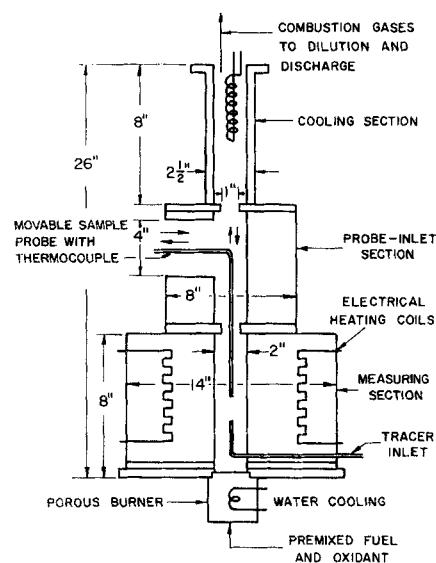


Fig. 1. Schematic diagram of a current form of the diffusion apparatus.

George Ember is with the American Oil Company, Whiting, Indiana.

Further details of the flat-flame burner are shown in Figure 2. Burner diameters of 2 and 3 in. have been used. For experiments carried out to date the fuel gas has been carbon monoxide or a mixture of carbon monoxide and hydrogen. The fuel is premixed with a slight stoichiometric deficiency of oxygen and with a diluent gas before being fed to the gas inlet of the burner. The diluent in the experiments described here is carbon dioxide, which serves to control temperature of the experiment. In measurements of binary diffusion coefficients the second gas may be added to the system as the diluent, though this has not been the case for the carbon dioxide-water system. The oxygen stream may be bubbled through water after it is metered. The trace of water thus added helps to stabilize the carbon monoxide flame, which is otherwise difficult to control, but does not significantly influence measured values of diffusivities.

The flame is stabilized on top of the sintered bronze plug in a very flat layer with a luminous part up to about  $\frac{1}{4}$  in. thick, the thickness depending upon the particular gas mixture used. Selection of material for the plug is somewhat critical; surface pore size must be quite uniform in order to produce a sufficiently flat flame, free of spikes or other disturbances. Good results have been obtained with grade-3, Porex porous bronze.

Copper tubing mounted in the plug carries cooling water. Sintered bronze must be cooled under the conditions employed here, otherwise further sintering occurs, with changes in pressure drop and flow pattern. The need for cooling coils determines the thickness of the plug required; a sufficiently laminar flow can be obtained with a much thinner porous plug. It is believed that the surface of the plug attains temperatures no higher than about  $250^{\circ}\text{C}$ . Even so the plugs have rather short and uncertain lifetimes before unfavorable velocity profiles result, and the burner is designed to allow ready replacement of the plug through the gas-inlet end of the burner.

Figure 3 illustrates details of the measuring section. Here the tracer is added, gas samples are taken, and temperatures are measured. Fuel, diluent, and oxidant rates to the burner are controlled to give velocities in the measuring section of 6 to 13 cm./sec. at room temperature, corresponding to 24 to 78 cm./sec. for the temperature range  $1,200$  to  $1,800^{\circ}\text{K}$ . These velocities in turn represent Reynolds numbers of 45 to 600 based on a measuring-section diameter of 3 in. The tracer inlet and the sample probe are (80/20) platinum-rhodium capillaries of 0.5 mm. I.D. Reynolds numbers based on this di-

mension are in the range 0.6 to 10. One expects laminar conditions for the cylindrical measuring section as a whole. There will tend to be slight disturbances about the horizontal section of the tracer inlet, which should disappear between the horizontal section and the tip of the tracer inlet, and boundary-layer effects at the inlet and probe tips. In addition slight free convection can occur if the tracer density is different than that of the bulk gas. Some of these effects have been investigated by Walker and Westenberg with careful hot-wire anemometer measurements. They conclude that provided the tracer-inlet velocity and the bulk-gas velocity are at least crudely matched, effects of the boundary layer and of slight mismatch between tracer and bulk-gas velocities very quickly dissipate because of the generally laminar nature of the bulk flow. In the present work it was observed that deviation in the velocities might be as much as 50% for self-diffusion experiments but no more than about 30% for binary diffusion before the experimental data were affected. The difference is attributed to free-convection effects in binary diffusion.

The measuring section has two separate electrical heating circuits in the wall. The inner wire is 60/40 platinum-rhodium (2 kva. maximum at 190 v.), and the outer is Kanthal A (up to about 1 kva. at 110 v.). The heat balance of the entire apparatus is strongly affected by the presence of the relatively cold porous burner at the bottom. The wall of the measuring section radiates at high rates to the burner, so that heat is conducted under quite steep gradients to the inner surface of the insulated wall from both the wall itself and the gas. The resulting temperature profile is indicated in Figure 4 for a typical situation. Despite these steep profiles in the gas stream there is commonly a cylindrical plug of gas at least 1 in. in diameter and 1 to 2 in. long just above the tracer inlet in which the extreme temperature variation is less than 1% of the local absolute temperature. This isothermal region is easily of ample size to provide the necessary number of gas samples for determination of diffusivities.

Temperatures are measured with platinum-rhodium thermocouples (94/6 and 70/30) mounted as shown in Figure 3. In some experiments these have been of two bead diameters so that estimates of the radiation correction to temperature readings could be made. Usually the radiation corrections have been made by calculation, with handbook values for the emissivity of platinum. Calculated corrections at up to  $1,400^{\circ}\text{K}$ . have been  $28^{\circ}$  to  $35^{\circ}\text{K}$ . and have been within about 5 deg. of the corrections estimated by extrapolating tempera-

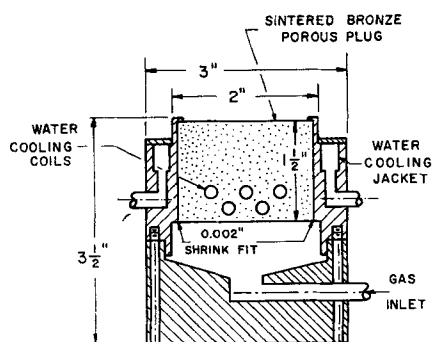


Fig. 2. Details of a current burner design.

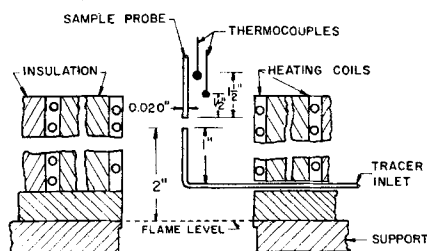


Fig. 3. Details of the measuring section.

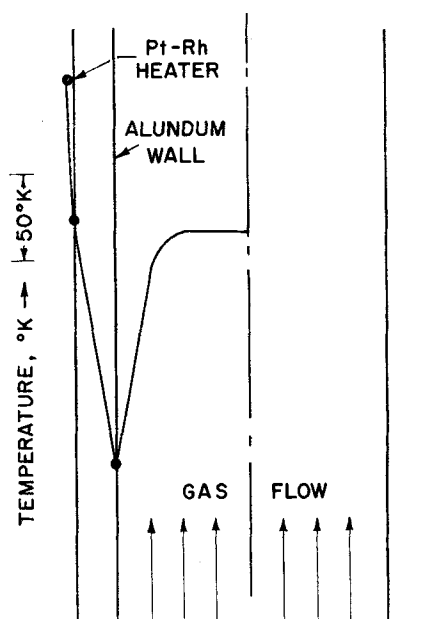


Fig. 4. Schematic diagram of the characteristic temperature profiles observed in the measuring section.

tures indicated by two thermocouples to zero bead diameter. Because of the slight axial temperature gradients in the measuring section temperature corrections for conduction along the thermocouple lead wires have been only about 5°K. at most. These corrections are sufficiently precise for diffusivity experiments, giving rise to uncertainties in local temperatures of about 1%. More elaborate precautions and corrections must be made in thermal conductivity experiments presently being carried out in equipment of similar type.

The sampling probe with attached thermocouples can be brought to a desired location by a three-dimensional positioning device having micrometer precision. Measurements are generally made on the axis of the apparatus from about 1 to 15 mm. above the tracer inlet capillary.

The probe inlet section is separated from the measuring section by an Alundum disk with a 1-in. diameter hole on the axis. The probe inlet section has a slit about 4 in. long and 1 in. wide through which the probe is inserted (note Figure 1). The vertical part of the probe consists of the sample capillary and the insulated thermocouples. A ceramic sleeve on the capillary helps to stiffen it. In the horizontal section of the probe the capillary passes through a water-cooled jacket so that the gas sample is cooled essentially to room temperature before being pulled into the analytical equipment.

Another Alundum disk separates the probe-inlet section from the chimney and cooling section. The combustion gases are cooled by the water coil shown in Figure 1, diluted to a safe radiation level, and exhausted outside the laboratory by two centrifugal blowers mounted in series. The first of these dilutes the combustion gases with laboratory air, and the second mixes a large volume of outside air with the exhaust gas before pushing it into the atmosphere. Choice of the blower sizes was governed by the need to comply with Atomic Energy Commission regulations for safe disposal levels for carbon-14. Locating one blower within the laboratory ensures that the chimney and cooling section will be under slight vacuum with respect to the laboratory. The laboratory in turn will be under slight vacuum with respect to adjacent rooms. The danger of release of radioactive gases or of carbon monoxide to the laboratory or to adjacent rooms is decreased in this way. As a further precaution in the event of possible poisoning of the laboratory air the operators wear respirators connected to a clean air supply during an experiment.

For experiments in which the fuel gas contained hydrogen and in which water was a product changes in the apparatus were necessary in the burner and in the chimney and cooling section. An additional cooling circuit was added to the burner around the gas-inlet line. Also the space below the porous plug was filled with crumpled stainless steel screen to act as a flame arrester. The chimney section indicated in Figure 1 was removed, and a condenser mounted at about 135 deg. from vertical was substituted. The condenser was fabricated from copper and had a counterflow water jacket and provision for injection of a water spray directly into the hot gas. The condensed water was diluted with additional water and discarded in a floor drain. The uncondensed gases were diluted and discharged from the laboratory by means of the dual blower arrangement described above.

Fuel gases and oxygen were high-purity grades metered by calibrated orifices. In the experiments for which results are given here two radioactive gases  $C^{14}O_2$  and  $CH_3T$  were used. Both were stored in small cylinders at relatively low pressure (200 to 400 lb./sq. in.). Each was diluted with bone-dry, non-radioactive gas to a convenient level of activity, 0.35  $\mu$ curies/ml. for carbon dioxide and 0.85  $\mu$ curies/ml. for methane. It was possible to meter the flow of the tracer gas to the apparatus by taking advantage of the radioactivity. That is when the tracer flow rate had been set at some value, the flow was diverted from the inlet capillary to the radioactive counting cell, where it was diluted with a known flow rate of an inert gas. The relatively large (2 to 4 liters/min.) flow rate of inert gas could be varied and the activity of the diluted flow observed. Activity of the undiluted tracer gas was known from a separate experiment, so that the quite small tracer flow could be calculated with good accuracy.

## Radioactivity Detection Systems

A gas sample, having been pulled through the sampling probe and cooled, flowed to a counting cell. Two such cells were used in the work reported here, and a third has been described previously (3). The first, used for detecting carbon-14 in pure carbon dioxide and in mixtures of carbon dioxide and water, was actually two detectors mounted on either side of a thin sample chamber. Two commercially available, teflon-insulated detectors were used. They were operated in the Geiger-Müller range at 1,350 v. with 99.05% helium, 0.95% isobutane as the counting gas. The sample chamber was made of acrylic plastic and was 1 in. in diameter and 2 mm. thick. The center was cut out to give a sample volume of about 1 ml. This center portion was separated from the counting cells by aluminized Mylar of about 0.7 mg./sq. cm. density. Stainless steel capillaries were mounted in the plastic so as to allow the gas sample to flow through the sample chamber.

The second counting device was an internal flow detector used primarily for detection of tritiated methane in carbon dioxide-methane mixtures. It operated satisfactorily in both the Geiger-Müller range (with 96% helium, 4% isobutane as counting gas) and the proportional range (with P-10—90% argon, 10% methane—as counting gas). Generally the former conditions were used.

With an internal detector one does not separate the sample gas from counting cell but mixes counting gas and sample gas in known proportion and allows the mixture to flow through the high-voltage region of the cell. This is necessary when detecting tritium because the relatively low-energy beta radiation from tritium would be rather highly absorbed in a aluminized Mylar film separating counting and sampling cells. The disadvantage in use of the internal flow detector is that the sample flow rate must be known accurately. Sample flow rates (about 1 ml./min.) were measured here by the soap-bubble method. A soap film was admitted to the sample line, and the time of its passage through a calibrated glass pipet was observed. This is a useful means for measuring very small flow rates, but the accuracy is no better than 5 to 10%. In the present case this became the limiting accuracy of the experiment when the internal flow detector was employed. More accurate means for detecting tritium are available but were considered too costly for use here.

## ANALYSIS OF THE DATA

The mathematical model of the diffusion process obtained with the device described here has usually been taken as that of the point source, and this model is used here. Assume isothermal and isobaric conditions for a system in which one component is present as a trace. Under these conditions and for steady, unidirectional flow the diffusion equation for the trace component in cylindrical coordinates takes the form

$$U \frac{\partial a}{\partial z} = D \left[ \frac{1}{r} \frac{\partial}{\partial r} \left( r \frac{\partial a}{\partial r} \right) + \frac{\partial^2 a}{\partial z^2} \right] \quad (1)$$

For convenience concentrations (designated by  $a$ ) are measured in units of disintegrations per second per unit volume.

Appropriate boundary conditions for the point-source model as represented in Figure 5 are

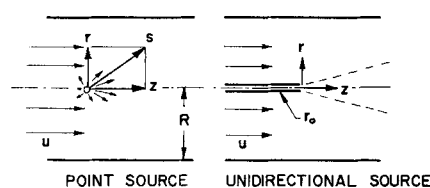


Fig. 5. Coordinate systems for the point-source and unidirectional-source models.

$$\lim_{s \rightarrow 0} \left[ -4\pi s^2 D \frac{\partial a}{\partial s} \right] = a_0 \left( \frac{T}{T_1} \right) q_1 \quad (2)$$

$$\lim_{s \rightarrow \infty} a = 0 \quad (3)$$

$$\left( \frac{\partial a}{\partial r} \right)_{r=0} = 0 \quad (4)$$

The solution satisfying Equations (1) to (4) may be found for example in Carslaw and Jaeger (4) and is as follows:

$$a(s, z) = \frac{a_0 q_1 T}{4\pi D s T_1} \exp [-(U/2D)(s-z)] \quad (5)$$

Along the axis of the measuring section, where  $s = z$ , this reduces to

$$a(z, z) = a_0 q_1 T / 4\pi D T_1 z \quad (6)$$

Hence one might obtain a value for  $D$  very conveniently by observing the slope of a plot of the reciprocals of concentrations measured along the axis versus distance along the axis. Actually, as is pointed out by Walker and Westenberg, the sampling probe draws its sample from a volume not necessarily centered about its tip. Furthermore penetration of the bulk gas stream by the tracer flow may translate the actual source position a small distance from the inlet tip. The actual (virtual) distance between source and sampling points should be used in a calculation of  $D$  from activity at a particular point, but the plot of reciprocal activity against either measured distance from the inlet tube or actual distance from the true source is linear and its slope can be used to calculate  $D$ .

It might be argued that a more realistic model of the experiment used here should treat the source as unidirectional, finite in diameter and located in a finite region, as is indicated in Figure 5. Boundary conditions for this case might reasonably be taken to be

$$a(r, 0) = a_0 [1 - H(r - r_0)] \quad (7)$$

$$(\partial a / \partial z)_{z=0} = 0 \quad (8)$$

$$(\partial a / \partial r)_{r=0} = (\partial a / \partial r)_{r=R} = 0 \quad (9)$$

The solution can be obtained readily by use of the Laplace and finite Hankel transforms in the form of a Fourier-Bessel series.

The equation for the unidirectional model is very awkward to apply. The diffusion coefficient appears implicitly, and the series solution converges rather slowly. All experimental evidence presently available supports the assumption that the point-source model represents the experiment quite adequately, perhaps because the bulk gas flow tends to elongate the point source in the direction of flow so that it more nearly resembles an unidirectional source than a point source. Walker and Westenberg in their first paper (2) give a good discussion of the experimental evidence in favor of the use of the point-source model. The linearity of reciprocal radioactivity measurements along the axis is excellent (2, 3).

#### EXPERIMENTAL RESULTS AT ROOM TEMPERATURE

It has been convenient to test performance of the apparatus at room temperature, with no flame, where a wider choice of diffusion systems can be made. Results for self-diffusion of carbon dioxide have been reported (3). Some experiments with the carbon dioxide-methane system are illustrated here.

Six kinds of experiments were carried out. These are as follows:

1.  $C^{14}O_2$  was allowed to diffuse as the tracer in otherwise pure carbon dioxide.
2.  $C^{14}O_2$  was used as tracer is equimolar carbon dioxide plus methane.
3.  $C^{14}O_2$  was used as tracer in pure methane.
4.  $CH_3T$  was used as tracer in otherwise pure methane.
5.  $CH_3T$  was used as tracer in equimolar carbon dioxide plus methane.
6.  $CH_3T$  was used as tracer in otherwise pure carbon dioxide.

Case 1 gives the self-diffusion coefficient  $D_{11}$  of carbon dioxide. This was a repetition of the experiments reported previously (3), but analyses in the present case were carried out with the less accurate internal flow detector, which was needed for detection of tritium. Case 1 served then to give a measure of the accuracy of the internal-flow detection system.

Similarly Case 4 gives the self-diffusion coefficient of methane  $D_{22}$ .

Cases 3 and 6 give values of the binary diffusion coefficients for the carbon dioxide-methane system in the limits of vanishingly small concentrations of the diffusing species. These cases then yield the coefficients  $D_{12}$  and  $D_{21}$ , respectively.

Cases 2 and 5 involve ternary systems of carbon dioxide, methane, and tracer, where the last is present in very small amount. The resulting diffusivities will be labeled  $D^{*1E}$  and  $D^{*2E}$ ; these are the trace diffusivities of the two components in an equimolar mixture. (Values of  $D_1^*$  and  $D_2^*$  will be functions of the concentration of the bulk gas, movement of the trace component being influenced differently by collisions with the different species of the bulk gas. Hence the subscript  $E$  is used to denote the equimolar concentration.)

The six diffusion coefficients are interrelated by the two approximate equations which follow:

$$1/D_1^* = x_1/D_{11} + x_2/D_{12} \quad (10)$$

$$1/D_2^* = x_1/D_{21} + x_2/D_{22} \quad (11)$$

Here  $x_1$  and  $x_2$  are mole fractions of the bulk-gas components. The above equations may be derived in several ways, for example from the Stefan-Maxwell equations for a ternary system in which one component is present as a trace (5).

For the equimolar system, where  $x_1 = x_2 = 0.5$ , one can derive a number of relationships among the various

TABLE 1. DIFFUSIVITIES IN THE SYSTEM:  
CARBON DIOXIDE (1)-METHANE (2) AT  
1 ATM. AND 297 °K., SQ. CM./SEC.

	Measured values	Computed from $D^{*1}$ and $D_{12}$ or from $D^{*2}$ and $D_{21}$	Computed from $D^{*1}$ , $D^{*2}$ and $D_{11}$ or $D_{22}$
$D_{11}$	0.0925(*) 0.0990	0.0939	0.0939
$D_{22}$	0.230 0.226	0.217	0.239
$D_{12}$	0.151 0.158		
$D_{21}$	0.153 0.156		
$D^{*1E}$	0.161 0.110		
$D^{*2E}$	0.123 0.188 0.178		

(\*) A more accurate value is believed to be 0.110 sq.cm./sec.

diffusion coefficients, assuming Equation (10) and (11) are valid. For example the self-diffusivities may be calculated from

$$D_{ii} = [(2/D^*_{iE}) - (1/D_{ij})]^{-1}$$

where  $i$  and  $j$  may be 1 or 2. Furthermore if  $D_{21} = D_{12}$ , which one expects to be at least very nearly true, a self-diffusivity can be calculated from the measured values of trace diffusivities  $D^*_{1E}$  and  $D^*_{2E}$  and the other self-diffusivity. That is

$$D_{ii} = [(2/D^*_{iE}) - (2/D^*_{jE}) + (1/D_{ij})]^{-1} \quad (12)$$

Measurements of all six characteristic diffusion coefficients then give one the opportunity to check Equations (10) and (11) as well as the equality of the binary coefficients  $D_{ij}$ .

Results of measurements and calculations are shown in Table 1 for 1 atm. and 297°K. The value of  $D_{11}$  shown is low compared with those previously measured at room temperature in the authors' work and by others (3). The more accurate value is 0.110 sq. cm./sec. The present error is that of the internal flow detection system and can be avoided by use of more sophisticated detectors.

Despite this discrepancy the six coefficients show good consistency and support the validity of Equations (10) and (11). The binary coefficients  $D_{12}$  and  $D_{21}$  are identical within the limit of experimental error. Walker, deHaas, and Westenberg (10) came to similar conclusions on the basis of measurements of binary and trace diffusivities.

#### HIGH TEMPERATURE TRACER DIFFUSIVITIES

Injection of  $C^{14}O_2$  into the combustion products from a carbon monoxide-hydrogen-oxygen-carbon dioxide flame yielded values of the tracer diffusivity  $D_1^*$  for the system carbon dioxide-water- $C^{14}O_2$  (trace). The relative amount of hydrogen in the fuel was varied so as to give gas mixtures with 10, 33, and 50% water in carbon dioxide. The relative amount of carbon dioxide added as diluent could be varied so as to control the temperature of the experiment.

It was decided to burn hydrogen to produce water in the gas stream rather than to add water vapor as a diluent because the former source gave much better control of the water content and eliminated the need for troublesome auxiliary equipment.

The relatively high burning rate with hydrogen as part of the fuel caused the flame to be much thinner than with pure carbon monoxide so that the porous burner tended to deteriorate more quickly unless flame temperature was kept rather low. On the other hand the high burning rate and thin flame permitted use of higher diluent concentrations so that it was possible to obtain lower temperatures with hydrogen added to the fuel.

TABLE 2. ISOTOPIC TRACER DIFFUSIVITIES OF  $C^{14}O_2$  IN MIXTURES OF CARBON DIOXIDE AND WATER

$T, ^\circ K. (D^*_{1E})_{x_2=0.1}$		$T, ^\circ K. (D^*_{1E})_{x_2=0.33}$		$T, ^\circ K. (D^*_{1E})_{x_2=0.5}$	
1,159	1.92	1,235	2.43	975	1.62
1,255	2.12	1,250	2.40	1,060	1.96
1,308	2.22	1,350	2.60	1,141	2.04
1,310	2.20	1,450	2.82	1,222	2.40
1,310	2.23			1,250	2.55
1,310	2.35			1,265	2.60
1,330	2.36			1,280	2.88
1,333	2.43			1,290	2.55
1,384	2.42			1,294	2.84
1,504	2.96			1,310	2.66
1,580	3.02			1,358	2.97
1,616	3.37			1,382	2.92

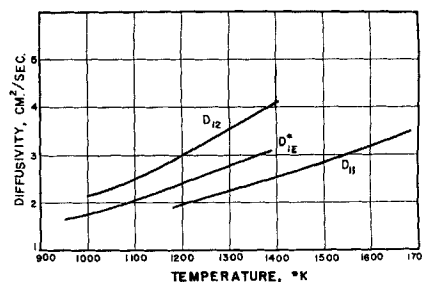


Fig. 6. Diffusivities in the carbon dioxide-water system.

In the equimolar water-carbon dioxide system therefore the temperature range 975° to 1,380°K. could be examined, compared with 1,160° to 1,616°K. with 10% water and 1,180° to 1,680°K. with pure carbon dioxide.

Radioactivity measurements were made with the sandwich cell for all three concentrations, and the internal-flow detector was also used with the equimolar mixture. Use of both cells allowed an estimate of the effect of condensed water on the accuracy of the counting method. No significant differences between the two experiments were observed, and both analytical methods showed about the same amount of experimental scatter. Probably this means that the sandwich cell lost some accuracy because of the presence of condensed water. One expects it to be normally more accurate than the internal-flow detection system because no measurement of sample flow rate is involved in its use.

Results of the experiments are tabulated in Table 2. Only a few values were obtained for 0.33 mole fraction water, most effort being concentrated on measurements in the equimolar mixture so that accurate calculations of  $D_{12}$ , the binary diffusivity, might be made from Equation (10). The plot of tracer diffusivities in the equimolar mixture was smoothed, and smoothed values of  $D_{11}$  from reference 3 were used. The calculated binary diffusivities are shown as the top curve in Figure 6. The middle curve represents smoothed trace diffusivities for carbon dioxide in the equimolar mixture, and the bottom curve is for self-diffusivity of carbon dioxide.

It is possible to make direct measurements of  $D_{21}$  in the present apparatus by diffusing tritiated water (HTO) in pure carbon dioxide. Such measurements have been made (5). These results require extensive additional discussion of experimental methods and will be reported in a separate paper.

It is interesting to observe the relative portions of the curves for  $D_{11}$ ,  $D^*_{1E}$ , and  $D_{12}$ . Such positions are consistent with Equations (10) and (11). One would expect curves for  $D^*_{2E}$  and  $D_{22}$  to be still higher and in the order listed. Such an ordering has indeed been observed: details will be reported in the publication referred to above.

Earlier measurements of self-diffusion coefficients (3) indicated that diffusion coefficients calculated from the Chapman-Enskog theory with the Lennard-Jones (12-6) potential and force parameters derived from viscosity data or from low-temperature diffusion data for carbon dioxide are lower than the observed values by 30 to 40% in the range, 1,200° to 1,700°K. This is illustrated in Figure 7 where the authors' self-diffusion data are compared with values predicted by the correlation of Kennedy and Thodos (6) which is based on a combination of low temperature experimental data and kinetic theory calculations.

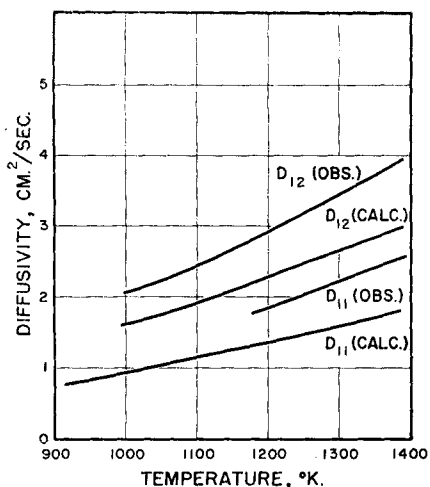


Fig. 7. Comparison of experimental results with theory; carbon dioxide-water system.

A similar comparison can be made for the binary-diffusion coefficient for the carbon dioxide-water system. Figure 7 shows such a comparison of the data of Figure 6 with binary diffusivities calculated from kinetic theory. The latter were calculated with the parameters of the Lennard-Jones potential obtained from high-temperature viscosity data and tabulated by Hirschfelder, Curtiss, and Bird (7), whose modified combining rules for binary systems with a polar component (8) were also used. Parameters for water were those of Rowlinson (9) obtained from experimental second virial coefficients. Again the calculated values are about 30% lower than the experimental ones. The differences can be accounted for at least approximately by assuming that the nonspherical shapes of the carbon dioxide and water molecules, particularly of the former, become significant in collisions at high temperatures when force fields of the molecules are rather deeply penetrated during collision (3).

## DISCUSSION

The apparatus described here must be considered to be still in the early stages of development. Results to date are uniformly favorable, and they confirm the feeling that the dynamic method is well suited to high-temperature measurements of diffusion coefficients.

There are disadvantages to the method. An experiment is rather expensive because of the large material flows used and somewhat difficult to carry out until one accumulates extensive experience with the equipment. The systems which can be studied are so far limited to those in which carbon monoxide is a convenient fuel. Probably other fuels can be used, but the necessary exploration of burner designs has not yet been carried out.

The maximum absolute temperature so far attained is about 50% higher than has been used previously. Maximum temperature of the present equipment is limited by the need to keep the relatively delicate bronze plug cool. Efforts to reduce this limitation are in progress. Greatly higher temperatures are not desirable for study of molecular transport properties however because difficulties connected with decomposition and excitation or ionization may arise. It is of more immediate interest to decrease the lower temperature limit of the apparatus, now about 1,000°K., so that better comparison with previous experimental data can be made.

Experiments in the use of the apparatus for measurement of thermal conductivities are currently in progress. This research is inherently more difficult at high temperatures because one needs to be so careful in controlling the

heat balance of the apparatus and in interpreting measured temperatures.

## CONCLUSIONS

The dynamic method, with high temperatures supplied by a flat flame and with use of radioactive tracer methods for analysis, has proved to be useful for accurate measurements of diffusion coefficients at high temperatures. Diffusion data obtained for temperatures of 1,000° to 1,700°K. have been sufficiently different than those calculated by kinetic theory to suggest that study of transport in this temperature range can contribute significantly to improvement and extension of the theory.

## ACKNOWLEDGMENT

The burner design shown in Figure 2 was worked out by Mr. T. A. Pakurar. This research was sponsored in part by Project Squid, which is supported by the U.S. Office of Naval Research under contract Nonr 1858(25) NR-098-038, and in part by the National Science Foundation, under grant G-19985.

## NOTATION

- $a$  = radioactivity, disintegrations per second per unit volume
- $D$  = diffusion coefficient, sq. cm./sec.
- $H(r - r_0)$  = heaviside unit step function; equals zero for  $0 \leq r \leq r_0$  and unity for  $r > r_0$
- $q$  = volumetric flow rate, cc./sec.
- $r$  = radial distance or coordinate, cm.
- $R$  = radius of the measuring chamber, cm.
- $s = (r^2 + z^2)^{1/2}$
- $T$  = absolute temperature, °K.
- $u$  = linear gas velocity, cm./sec.
- $x$  = mole fraction
- $z$  = axial distance or coordinate, cm.

## Subscripts

- $o$  = tracer inlet condition
- $1$  = datum temperature or volumetric flow at  $T_1$
- $1$  = component 1 (carbon dioxide in all specific cases)
- $2$  = component 2 (either methane or water)
- $11$  or  $22$  = self-diffusion coefficient
- $12$  or  $21$  = binary-diffusion coefficient for diffusion of a trace of 1 through 2 (or vice versa)
- $E$  = equimolar mixture.

## LITERATURE CITED

- Klibanova, T. M., V. V. Pomerantsev, and D. A. Frank-Kamenetskii, *J. Tech. Phys., USSR*, **12**, 14 (1942).
- Walker, R. E., and A. A. Westenberg, *J. Chem. Phys.*, **32**, 436 (1960); **29**, 1139, 1147 (1958).
- Ember, George, J. R. Ferron, and Kurt Wohl, *ibid.*, **37**, 891 (1962).
- Carslaw, H. S., and J. C. Jaeger, "Heat Conduction in Solids," pp. 266-267, Oxford University Press, England (1959).
- Ember, George, Doctoral thesis, Univ. Del, Newark, Delaware (1962).
- Kennedy, J. T., and George Thodos, *A.I.Ch.E. Journal*, **7**, 625 (1961).
- Hirschfelder, J. O., C. F. Curtiss, and R. B. Bird, "Molecular Theory of Liquids and Gases," p. 1111, Wiley, New York (1954).
- Ibid.*, p. 600.
- Rowlinson, J. S., *Trans. Faraday Soc.*, **47**, 120 (1951).
- Walker, R. E., N. deHaas, and A. A. Westenberg, *J. Chem. Phys.*, **32**, 1314-1316 (1960).

Manuscript received March 29, 1963; revision received June 14, 1963; paper accepted June 27, 1963. Paper presented at A.I.Ch.E. New Orleans meeting.